Sensors & Actuators: B. Chemical 407 (2024) 135468

Contents lists available at ScienceDirect

Sensors and Actuators: B. Chemical

journal homepage: www.elsevier.com/locate/snb

Activating the SERS features of screen-printed electrodes with thiocyanate for sensitive and robust EC-SERS analysis

Rebeca Moldovan [a], Martin Perez-Estebanez [b], Aranzazu Heras [b], Ede Bodoki [a,*], Alvaro Colina [b,*]

[a] Analytical Chemistry Department, Faculty of Pharmacy, Iuliu Haţieganu University of Medicine and Pharmacy, 4, Louis Pasteur, 400349 Cluj-Napoca, Romania
[b] Department of Chemistry, Universidad de Burgos, Pza. Misael Bañuelos s/n, E-09001 Burgos, Spain

ARTICLE INFO

Keywords:
EC-SERS
Spectroelectrochemistry
Substrate activation
Thiocyanate
Sensor
Propranolol

ABSTRACT

This study presents a novel electrochemical (EC) methodology for activating the SERS features of disposable silver screen-printed electrodes (AgSPEs) using a pseudohalide as a precipitating agent to guide the assembly of a nano-filamentous silver network responsible for a strong SERS enhancement. To the best of our knowledge, the use of thiocyanate for SPEs activation for quantitative purposes has not been reported before. In order to better study this complex system, time-resolved (TR) operando spectroelectrochemistry (SEC) measurements were performed by SERS and UV-Vis and correlated with SEM imaging of the electrode surface at different steps. Moreover, to significantly increase the reproducibility of the assays, a rapid EC protocol was proposed for the first time to obtain a reliable Ag/AgSCN reference electrode (RE) and a comprehensive optimization process was conducted to determine the critical parameters. Additionally, propranolol, as an emerging pharmaceutical pollutant has been selected as a model molecule to demonstrate the applicability of the method for rapid (3 min) quantitative analysis in the nM range from real river and tap water samples.

1. Introduction

Raman SEC is making progress in the field of analytical chemistry, holding great promise in bridging the gap between laboratory-based techniques and practical on-field applications [1]. Studies show that the EC potential has a strong effect on SERS measurements, influencing both the electromagnetic (EM) and the chemical (CM) mechanisms [2,3]. EC polarization of the SERS substrate has proved to modulate controlled adsorption of target molecules, bring higher specificity, higher sensitivity and other benefits [4,5]. EC-SERS has proved to be a robust and fast analytical technique for the detection of a wide variety of analytes [1], being one of the most promising analytical techniques in the near future [4]. The existence of ready-to-use SPEs substrates increases the accessibility and feasibility of these methods for cost-effective implementation on a larger scale. These ceramic plates already include all three electrodes that are needed for SEC measurements. Working electrodes (typically Ag, Au or Cu relevant for SERS) are not suitable for sensitive SERS analysis, but an atomic restructuring of the surface (activation) can be easily performed in a fast and reproducible way using EC oxidation and reduction steps. The EC activation of the AgSPEs substrates can also take place in the presence of the analyte, in-situ [6,7], leading to better control over the experimental environment, better reproducibility and higher sensitivity. Additionally, the fast generation of fresh and disposable SERS substrates, avoids probable long-term stability issues.

A limited number of analyte-targeted in-situ activation procedures using commercially available AgSPEs have been reported up to date for the successful detection of fentanyl [8], naratriptan [9], folic acid [10], $[Ru(bpy)_3]^{2+}$ [6] and ferricyanide [6]. The EC method was optimized in each study with respect to the target analyte, since some parameters significantly influence the resulted nanostructures and their interaction with the analyte. Further exploration is required to fully comprehend the impact of different variables on the resulted SERS substrates, including the pH, the presence and concentration of a precipitating

Abbreviations: AgSPEs, silver screen printed electrodes; BRB, Britton Robinson buffer; BSEC, bidimensional spectroelectrochemistry; CM, chemical; CV, cyclic voltammetry; EC, electrochemistry; EC-SERS, electrochemistry - surface enhanced Raman spectroscopy; EM, electromagnetic; LOD, limit of detection; LOQ, limit of quantification; MIPs, molecular imprinted polymers; Pseudo-RE, pseudo-reference electrode; RE, reference electrode; RSD, relative standard deviation; SEC, spectroelectrochemistry; TR-Raman SEC, time-resolved Raman spectroelectrochemistry.

* Corresponding authors.
E-mail addresses: bodokie@umfcluj.ro (E. Bodoki), acolina@ubu.es (A. Colina).

https://doi.org/10.1016/j.snb.2024.135468
Received 3 October 2023; Received in revised form 1 February 2024; Accepted 6 February 2024
Available online 8 February 2024

agent, as well as the specific EC technique employed. It has been established that the role of the counter anions present in solution is crucial [7]. Martín-Yerga et al. [7] studied the effect of different electrolytes for the analysis of ferricyanide on AgSPEs. They observed that the activation in the presence of Cl^- leads to 9 times higher enhancement of the Raman signal compared to activation in the presence of weakly or noninteracting anions with the metallic electrode surface, such as NO_3^-. For this reason, Cl^- in different concentrations was mostly used as precipitating agent in previously reported studies [6,8–10]. The influence of Br^- [11] was reported in one study where AgSPEs were activated in oxidation (EC-SOERS) for the analysis of clopyralid in tap water. Pseudohalides, such as SCN^- have not yet been explored as a supporting electrolyte component for SERS enhancement for quantitative purposes. Through the S and N atoms, it demonstrates strong affinity towards silver, chemisorbing onto its surface in a S-bound, N-bound or bridge bound manner [12,13]. In various steps of the Raman SEC experiments, complex chemical (chemisorption, precipitation, complexation) and physical (physisorption) interactions with the electrode surface may occur, able to significantly contribute to the generation of a good SERS substrate for the detection of the target analyte.

Propranolol, a β-blocker commonly used for treating various cardiovascular conditions, was selected as a model molecule. The extensive therapeutic use of these substances is accompanied by a significant release into the environment [14] posing risks to ecosystems and aquatic organisms [15]. Propranolol, detected in various environmental compartments (up to 2.27 nM in rivers [16]) is prioritized for worldwide environmental monitoring [17,18]. Additionally, sources of drinking water may be contaminated with potential acute or chronic toxicity towards humans [19]. Liquid chromatography coupled with mass spectrometry is the standard technique employed for the detection of β-blockers [19,20], but routine monitoring is problematic, requiring centralized analysis and highly skilled personnel. Hence, more accessible techniques, such as EC-SERS, are investigated for on-site environmental monitoring [21].

In this work, in-situ and operando SEC techniques are used to develop a method for quantification of propranolol (Fig. 1). In this regard, a new methodology for activation of SERS features on disposable AgSPEs is proposed using for the first time KSCN as precipitating agent. To the best of our knowledge, up to now pseudohalides have not been explored for activation of SPEs for quantitative purposes. The optimized TR-Raman SEC has been employed to successfully quantify propranolol in the nanomolar range in a simple, fast, sensitive and selective manner from spiked river and tap water samples with no pretreatment needed, other than a simple filtration for turbid river samples. Additionally, FE-SEM and EDX surface imaging and time-resolved UV–VIS SEC has been employed to gain a better insight on the processes occurring during the TR-Raman SEC measurements.

2. Materials and methods

2.1. Reagents and solutions

(±) Propranolol hydrochloride (≥99%), perchloric acid ($HClO_4$, 60%), boric acid (≥99.5%), phosphoric acid (≥85 wt% in H_2O), acetic acid (≥99%) and potassium chloride (>99.0%) were purchased from Sigma-Aldrich (St. Louis, USA). Potassium thiocyanate (KSCN, 99%) was acquired from VWR International (Pennsylvania, USA) and lithium perchlorate ($LiClO_4$, > 99%) from ACROS Organics (Geel, Belgium). Sodium hydroxide (99.3%) was purchased from Lachner (Neratovice, Czech Republic). All reagents were analytical grade and used as received

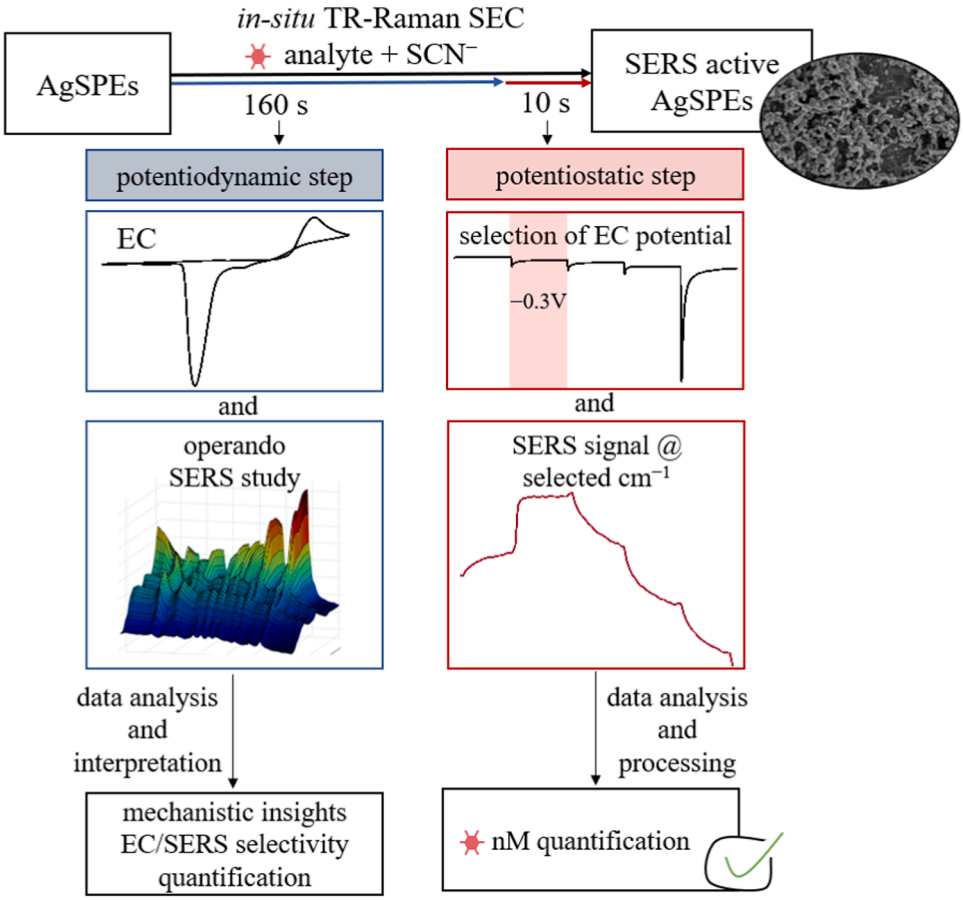

Fig. 1. Scheme of analytical principle.

without further purification.

All solutions were prepared using high purity water acquired from a Milli-Q® Direct Water Purification System, supplied by Millipore (18 MΩ·cm resistivity at 25 °C).

2.2. Instrumentation and electrodes

TR-Raman-SEC instrumentation consisted of a customized SPELEC-RAMAN device (Metrohm-DropSens, Spain) equipped with a 785 nm laser source. A Raman probe (DRP-RAMANPROBE, Metrohm-DropSens, Spain) was connected to this instrument. For the experimental procedures, a custom-made cell designed for SPEs was employed. The instrument was controlled using DropView SPELEC software (Metrohm-DropSens), enabling real-time and synchronized spectroelectrochemical data acquisition.

Metrohm-DropSens AgSPEs (AgC013) were used for the EC-SERS experiments. They consist of a 1.6 mm silver working electrode, a carbon auxiliary electrode and a silver pseudo-reference electrode (pseudo-RE). To improve the reproducibility for calibration and problem samples, it was necessary to modify the pseudo-RE before the experiments. In order to do this, a current of 100 μA was applied for 5 s to the pseudo-RE in a blank solution of 0.1 M $LiClO_4$ and 10 mM KSCN. After the procedure, the electrode was rinsed with ultrapure water and it was let to dry. Thus, a stable RE of Ag/AgSCN was established.

2.3. TR-Raman-SEC measurements

DropView SPELEC software was used for TR-Raman-SEC measurements to record both the Raman spectra and the EC information simultaneously in a synchronized manner. The laser output power throughout the measurements was 262 mW if not otherwise stated. An integration time of 1 s was applied across all TR-Raman-SEC experiments. The electrochemical technique used to roughen AgSPEs for TR-Raman-SEC experiments was cyclic voltammetry (CV). All potentials are referred to Ag/AgSCN RE if not otherwise stated. A CV was applied between –0.50 and +0.30 V, starting at –0.10 V in anodic direction for 2 cycles. Unless otherwise stated, a scan rate of 0.02 V s^{-1} and a step potential of 2 mV were used for the electrochemical measurements. The TR-SEC measurements were conducted at ambient temperature, adding 50 μL working solution on the AgSPEs.

2.4. Surface characterization

The morphology of the activated substrates was studied using an ultra-high-resolution Field-Emission Scanning Electron Microscope (FE-SEM), model GeminiSEM560 (Zeiss), applying an electron beam of 2.00 kV and collecting the response of the secondary electrons with an in-lens or a lateral detector.

In order to characterize the substrate at every step, four SEM images were taken during the optimized activation CV at the two upper vertexes and the two lower vertexes. The CV procedure was applied on 4 electrodes in blank solution and stopped at the following potentials: +0.30 V (first cycle), –0.5 V (first cycle), +0.30 V (second cycle) and –0.50 V (second cycle) respectively. The electrodes were rinsed with ultrapure water and analyzed to observe the structures that are formed in oxidation and reduction steps.

Energy-dispersive X-ray (EDX) spectroscopic measurements were took using the equipment coupled to the FE-SEM equipment previously described, using the detection system X Ultim Extreme (Oxford Instrument), with active area of 100 mm^2.

Processes that take place at the surface of the electrode and in solution during the activation CV were investigated by UV–VIS bidimensional spectroelectrochemistry (BSEC). For these measurements, a bifurcated optical fiber (QBIF600-UV–VIS, Ocean Optics) was connected to a deuterium light source. For normal configuration experiments, a reflection probe consisting of 6 illumination optical fibers and a central collection optical fiber (FCR-7UV200–2–2.5 ×100-ME-SR, Avantes) was connected. The reflection probe was positioned with the help of the home-made cell [22]. For parallel configuration measurements, two bare optical fibers with a diameter of 100 μm (Ocean Optics) were positioned facing each other on the surface of the working electrode (Ag010, Metrohm-DropSens) at a distance of 0.2 mm. One of the optical fibers was connected to the light source, while the other was connected to the spectrometer. In order to perform the experiments, 50 μL of solution was placed on the surface, covering the three-electrode system as well as the ends of the reflection probe and the bare optical fibers. The spectra recorded in the initial solution served as the reference spectrum for all experiments. Metrohm-DropSens silver electrodes (Ag010), fabricated in the same manner [23] were used for these experiments because of the higher surface area of the working electrode (4 mm). This allowed an easier integration with the setup for BSEC measurements.

2.5. Quantitative analysis

The applicability of the developed SEC methodology has been tested on tap and river (filtered) water samples spiked with propranolol. Spiked samples were prepared in ultrapure water at concentrations of 15 and 30 nM propranolol, using the stock solution of the standard. River water was collected from Arlanzón river, Burgos (42°20'15.1"N 3°42'40.2"W) and used in the same day after a simple filtration using regular filter paper in order to remove large visible constituents. River and tap water samples were diluted in a 1:1 ratio with the electrolyte and precipitating agent.

For quantitative purposes, the intensity of the characteristic Raman band of propranolol at 1367 cm^{-1} was monitored. The data collected during the activation CV procedure (potentiodynamic step) and after it (potentiostatic step) were compared at –0.30 V (vs. Ag/AgSCN) in terms of sensitivity and reproducibility. The SERS intensity of propranolol was extracted from the spectra collected at 150 s for the potentiodynamic step, whereas for the potentiostatic step, an average of the Raman intensity at 1367 cm^{-1} was calculated from 3 to 10 s, considering that in the first 2 s the equilibration of the system is still taking place. The estimated limit of detection (LOD) was calculated based on the slope of the calibration curve (n = 3) and the standard deviation of the response.

3. Results and discussion

3.1. In-situ potentiodynamic activation of AgSPEs

The Raman SEC response of 1 μM propranolol during the EC activation of AgSPEs is illustrated in Fig. 2 A. The main characteristic Raman bands of propranolol [24,25] at 1367 cm^{-1} and 1565 cm^{-1} corresponding to stretching C-C vibrations and bending C-H vibrations of the naphthalene ring (Fig. S1A) are highly enhanced during the formation of the SERS substrate. The evolution of the Raman signal of propranolol during the SEC experiment, has been monitored as voltaRamangram at 1367 cm^{-1} along with the EC signal (Fig. 2B).

The voltametric procedure is conducted in anodic direction starting from –0.10 V (vs. Ag/AgSCN). During the SEC experiment involving two CV cycles, several processes can be identified. In the first anodic scan, a well-defined peak around +0.18 V is observed, corresponding to the oxidation of the silver electrode surface with the immediate precipitation of the Ag^+ to AgSCN ($K_{sp} = 1.03 \times 10^{-12}$). Depending on the used KSCN concentration, the reaction may continue with the formation of soluble Ag^+ complexes [26,27], such as $[Ag(SCN)_2]^-$. In the cathodic scan of the first cycle, the formerly generated silver salts and complexes are reduced to metallic silver nanostructures at around –0.20 V and –0.05 V respectively. In the second cycle, the metallic silver is once again oxidized with distinctive anodic peaks for Ag^0 nanostructures previously generated (at +0.09 V) and bulk silver (+0.15 V). This difference is because Ag^0 nanostructures require less energy to be oxidized. Similar to the first cathodic scan, in the second cycle, once again the

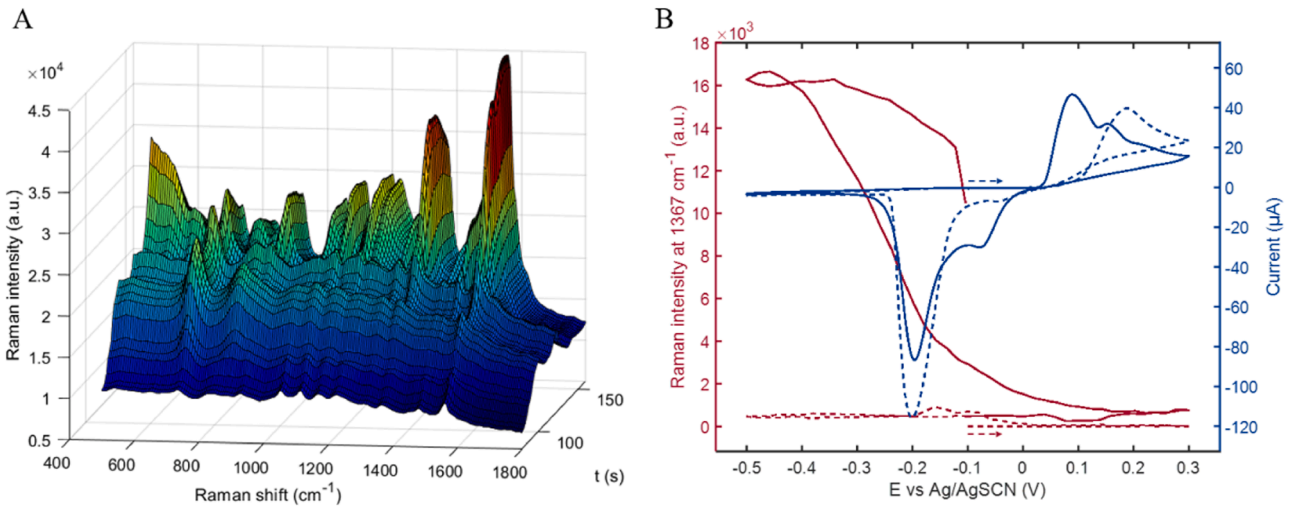

Fig. 2. 3D Surface plot showing the evolution of the Raman signal of propranolol for the second CV cycle on AgSPEs (A) and CV (blue) and voltaRamangram at 1367 cm^{-1} (red) during the first (dashed line) and second (solid line) CV cycles (B). Measurement conditions are 0.1 M $LiClO_4$, 10 mM KSCN and 1 μM propranolol.

reduction of various forms of silver compounds is recorded. At this point, a great enhancement of the Raman signal of propranolol is observed (Fig. 2 A, red solid line Fig. 2B), due to the adsorption of this analyte on the electrosynthetized Ag SERS substrate. Although propranolol is known to strongly adsorb on noble metal surfaces [28], within the studied potential range, no EC interference was expected as its oxidation is occurring above +0.90 V (vs. Ag/AgCl) [28]. Different concentrations of propranolol tested during activation demonstrated that the analyte does not interfere with the aforementioned processes at concentrations up to 0.5 μM (Fig. S1B). Nevertheless, at concentrations above 1 μM propranolol, the EC processes are slightly hindered (data not shown).

To the best of our knowledge, this is the first time that the use of SCN^- is proposed for the modification of Ag electrodes in EC-SERS experiments for quantitative purposes. It is worth mentioning that when similar experiments were performed using chloride as precipitating agent at 0.1 M, the signal for 1 μM propranolol was absent (data not shown), which makes the presented strategy outstand in comparison with classical ways to generate EC-SERS substrates. To further study the SCN^- modified system, the surface modifications at key points of the SEC experiment have been monitored by SEM and EDX analysis. After the first oxidative step (+0.30 V) a relatively uniform dendritic coverage of the electrode with densely formed AgSCN precipitate is observed in the SEM micrograph (Fig. 3A). The presence of the silver salt is confirmed also by the EDX analysis by the emerging peaks of S and N atoms (Fig. S2A). The subsequent reduction step leads to the formation of heterogeneous clusters of Ag^0 nanostructures from AgSCN with sizes that do not surpass 100 nm (Fig. 3B). A significantly different surface morphology is observed after the second oxidative step with the formation of a rougher surface with AgSCN covered elongated nanostructures (Fig. 3C, Fig. S2B). The progressive nanostructuring of the surface will eventually lead in the last reduction step to the formation of a dense 3D network of filiform Ag^0 nanostructures (Fig. 3D) potentially

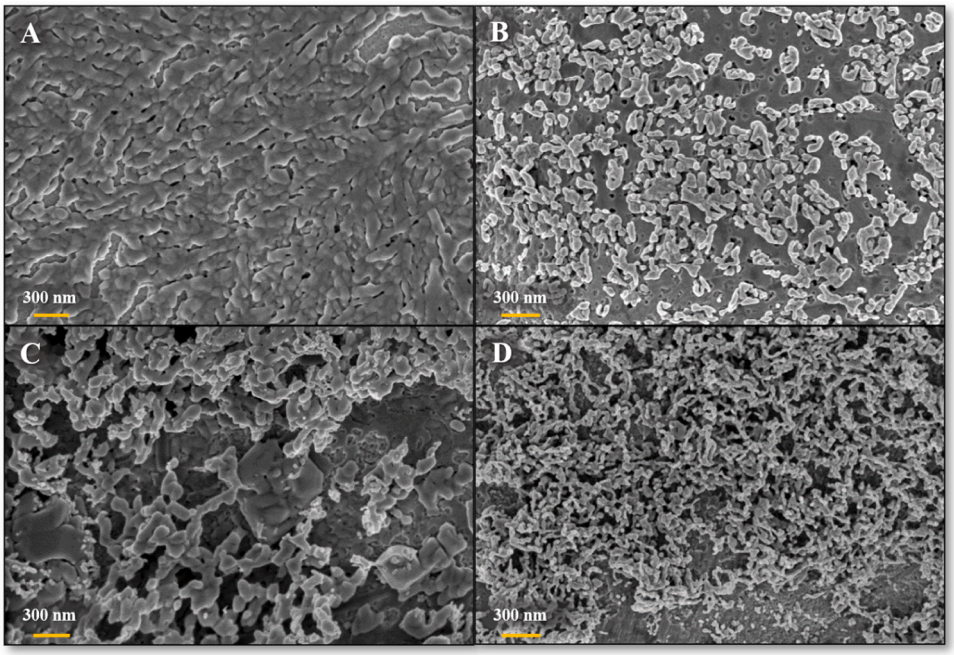

Fig. 3. SEM images of the AgSPEs surface during activation at the two upper vertexes and two lower vertexes of the EC procedure: +0.30 V (first cycle) (A), –0.50 V (first cycle) (B), +0.30 V (second cycle) (C) and –0.50 V (second cycle) (D).

capable of entrapping the analyte at numerous hot spots with increased SERS activity. Thiocyanate as a precipitating agent, besides limiting the Ag^+ loss during the oxidative steps, through the formation of a multi-layered covalently-bridged AgSCN chain networks [29,30], guides the electrogeneration of the filamentous silver network during the cathodic steps, favoring a high EM enhancement.

Significant Raman signal enhancement for propranolol is expected to occur during the noble metal nanostructuring taking place in the reduction steps. Due to an incipient phase of the nanostructuring taking place in the first cathodic scan, only a slight increase in intensity of propranolol band at 1367 cm^{-1} (Fig. 1B) can be observed. However, during the second cathodic scan, along with the maturation of the metallic network, a continuous and significantly (35-fold) higher signal increase emerged, showing an absolute maximum at about –0.45 V. A similar concentration-dependent SERS enhancement profile has been observed also for the other clearly distinguishable bands of propranolol at 395 cm^{-1}, 927 cm^{-1} and 1565 cm^{-1} (Fig. S1A) out of which the former two could not be allocated to a specific moiety or type of interaction based on the current band assignment from the literature.

The evolution of the characteristic Raman bands of SCN^- [31] was also monitored at 225 cm^{-1}, 450 cm^{-1} and 2114 cm^{-1} (Fig. S1A), bands attributed to stretching Ag-S and Ag-N vibrations, NCS angle bending and stretching C≡N vibrations respectively. These bands present similar behavior. During oxidation, a slight increase of the signal is observed (Fig. S3) due to their binding to the electrogenerated Ag^+ in the close proximity of the electrode. During the cathodic nanostructuring of the substrate, a further increase of the Raman intensity is occurring up to approx. –0.17 V due to the significant contribution of the EM enhancement. At the same time, the rising Raman band around 2070 cm^{-1}, attributed to free SCN^- ions further supports the dissolution of the silver precipitate [30]. Continuing the cathodic scan, the signal drops again due to molecular reorientation [12,13] and the built-up of excess electrons at the electrode interface that weaken the Ag – thiocyanate bond [30]. Similar pattern is observed for the second cycle at a higher magnitude due the continuous maturation of the metallic nanostructured network.

TR-UV-Vis bidimensional SEC analysis [22] was also performed in the same experimental conditions in order to better understand the mechanisms involved in the activation process. This method involves two spectroscopic setups, namely normal and parallel arrangements, operating simultaneously. While a light beam samples the system perpendicularly to the working electrode surface, another light beam passes through the solution parallel to the electrode surface. Consequently, this yields one EC and two spectroscopic signals for the same EC process. As a result, BSEC allows for the distinction of processes occurring in the solution and those occurring on the electrode surface during an EC reaction within a single experiment. Fig. S4 shows the recorded spectra (Fig. S4A and B) and the voltammogram together with the concomitantly obtained voltabsorptograms in normal (Fig. S4C and D) and parallel (Fig. S4E and F) configuration. First and second potential cycles are plotted separately for a better understanding of the process. Therefore, the change of absorbance is recorded for the two arrangements. A wavelength of 425 nm has been selected to describe the response in normal configuration because it is typically related to silver plasmonic nanostructures. For this system, the a very broad band is observed in the region between 320 and 450 nm (Fig. S4A), indicating that not well-defined geometries are obtained for the Ag nanostructures, in good agreement with the recorded SEM images (Fig. 3). For parallel configuration, 230 nm has been selected to describe the behavior of the system because it is related to SCN^- absorption [32], Fig. S4B. It is noteworthy, that in parallel configuration neither silver ion nor silver thiocyanate complexes are detected in solution during the oxidation step, only when the applied potential is higher than +0.30 V, the silver thiocyanate complexes are detected. As can be observed in Fig. S4C, during the first cycle, the absorbance in the voltabsorptogram in normal configuration increases during the oxidation of the electrode surface (around +0.15 V) due to the generation of AgSCN precipitate, in good agreement with the SEM images (Fig. 3A). During the reduction to Ag^0, a fast growth of the absorbance takes place (around –0.2 V) due to surface nanostructuring. Simultaneously, the evolution of the absorbance in parallel configuration can be analyzed (Fig. S4E). As can be seen, the absorbance decreases during the oxidation of the silver electrode because the concentration of SCN^- is decreasing in the diffusion layer. When the reduction of the precipitate takes place, during the cathodic scan, an increment of absorbance is observed due to the releasing of SCN^- from the crystals to the diffusion layer. A similar behavior is observed in the second cycle, with the mention that in normal configuration, a decrease of the absorbance is observed during the oxidation step due to the dissolution of silver nanostructures. However, the value of the absorbance at the anodic vertex potential is higher than the one attained in the first cycle, because of a higher amount of precipitate present in a more nanostructured manner (Fig. 3C). In the cathodic vertex potential, a higher value of absorbance in normal configuration is reached due to the maturation of the nanostructured matrix observed in the SEM images (Fig. 3D). The progressive darkening of the electrode surface at the different stages of the CV can also be visually observed (Fig. S5).

3.2. SEC optimization for propranolol detection

EC generation of SERS active substrates is significantly affected by various easily controllable parameters, such as the EC technique, electrolyte composition or precipitating agents. Diverse nanostructured surfaces are formed by varying these parameters, with differences regarding shape, size, density [7] and overall surface charge that could modulate their interfacial interaction (physisorption, chemisorption [33], complexation, etc.) with specific analytes. In this context, several key parameters such as electrolyte, KSCN concentration and upper vertex potential during CV were investigated and optimized for propranolol detection.

In order to avoid confusing surface effects, the nature of the electrolyte has to be carefully selected from those that do not present specific adsorption on silver surface, such as SO_4^{2-}, NO_3^-, F^- and ClO_4^- [34]. In our study, the enhancement of propranolol's Raman signal was monitored during the SEC experiments in 0.1 M $HClO_4$ (pH 1) and 0.1 M $LiClO_4$ (pH 6.1). The concentration of KSCN and the EC parameters were fixed for comparison. In both cases, the Raman signal enhancement for propranolol was greater in the second CV cycle, but it was at least two times higher in the presence of $LiClO_4$ (Fig. S6). The pH and counterions [35] of the tested electrolytes could affect the morphology of the generated nanostructures and their physicochemical interaction with the analyte. Therefore, $LiClO_4$ was selected and used as supporting electrolyte for the following experiments.

The influence of different concentrations (1–25 mM) of KSCN over the Raman signal enhancement of propranolol was also investigated (Fig. 4) while keeping all other parameters fixed. Increasing concentrations of the pseudohalide may influence the fraction of soluble silver complexes in the oxidative steps, the rate, yield and morphology of the forming nanostructured silver network as well as the adsorption-desorption processes during the cathodic scan. All voltametric peaks involving the transition of $Ag^0 \rightarrow Ag^+$ and $Ag^+ \rightarrow Ag^0$ respectively are positively correlated with the increase of KSCN concentration (Fig. 4A and Fig. 4B). Interestingly, a dichotomic behavior in the evolution of the SERS signal of propranolol over the two CV cycles (Fig. 4C) dependent on the low (< 5 mM) or high (> 5 mM) levels of the precipitating agent is observed. At low KSCN levels (1 mM) the highest Raman enhancement for propranolol is recorded during the first CV cycle, whereas at rising concentrations of the pseudohalide (above 5 mM) the trend is changing, achieving the highest spectroscopic signals during the second CV cycle. Obviously, for quantitative purposes experimental conditions offering the highest sensitivity with acceptable intermediate precision is desired, choosing 10 mM as optimum KSCN concentration for further

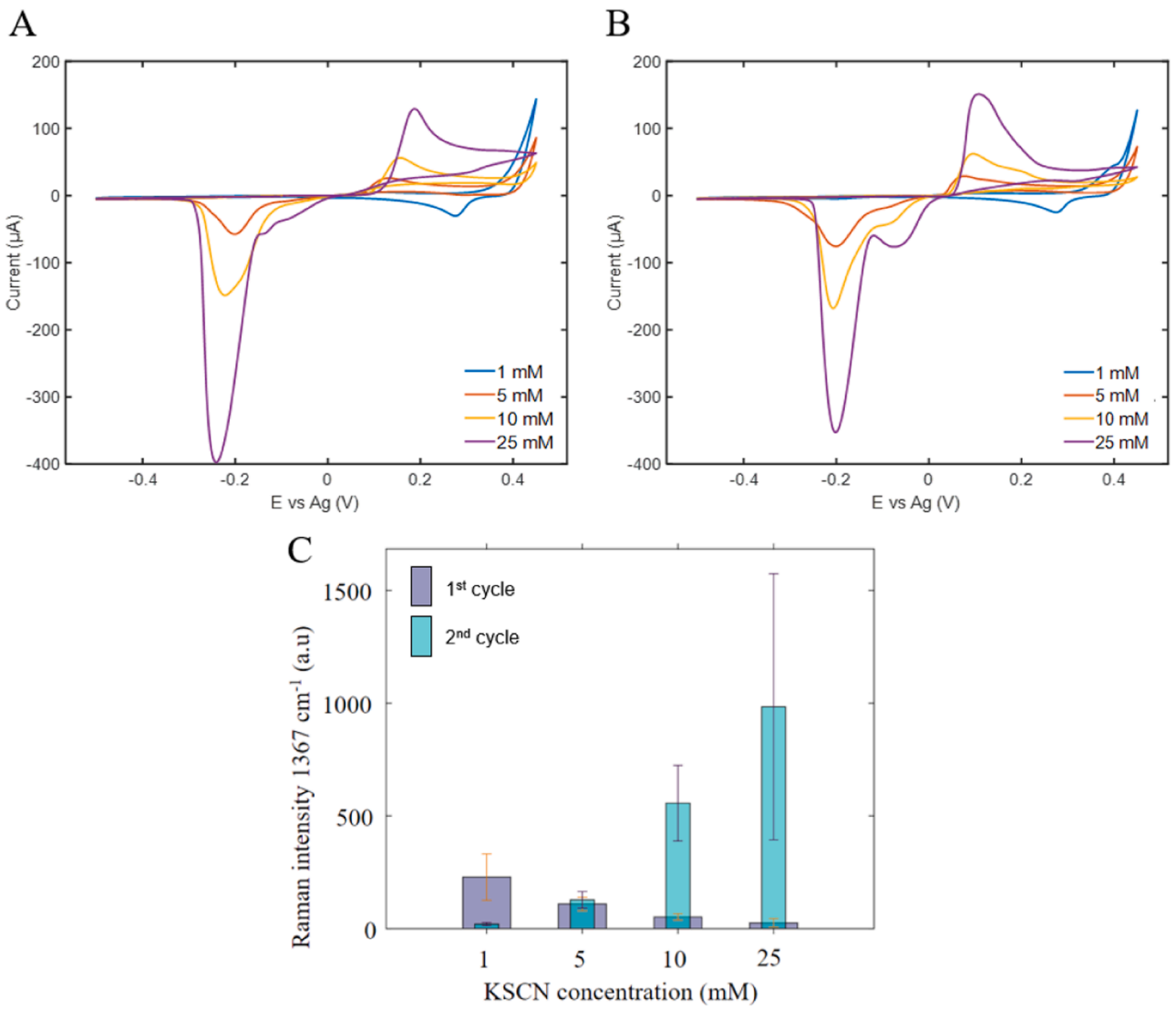

Fig. 4. First (A) and second (B) cycles of the potentiodynamic activation in the presence of different KSCN concentrations. Raman intensity at 1367 cm^{-1} during the SEC experiments (C). For a more accurate comparison, the Raman intensity was represented as an average of signal during 15 s of the anodic scan, for both cycles from –0.50 V to –0.20 V. Measurement conditions are 0.1 M $LiClO_4$ and 0.5 μM propranolol.

assays. Critically low KSCN concentrations ($\leq$ 1 mM) should be avoided since lower amounts of resulting AgSCN precipitate will not be able to prevent massive electrolytic silver dissolution and significantly limits the metallic nanostructuring of the electrode. Under such experimental conditions, the SEC profile tends to approach the behavior reported in presence of anionic electrolyte components forming soluble silver salts [7], such as NO_3^-.

Since the density and morphology of the AgSCN nanostructures formed in the oxidation step is crucial for the generation of the SERS substrate, the position of the upper vertex potential was modulated between +0.20 and +0.40 V with KSCN concentration fixed to 10 mM. No difference is observed in the enhancement pattern of propranolol's SERS signal. In all cases, the signal amplification of propranolol occurred in the cathodic scan of the second CV cycle. Differences were observed only for the intensity of the signal (Fig. 5A), the highest value being recorded using +0.30 V as upper vertex potential. Nevertheless, if the upper vertex reached +0.60 V accompanied by massive silver dissolution (Fig. 5B), the highest signal amplification was observed in the first CV cycle. Still, the signal is 17 times lower than in the optimum conditions (+0.30 V upper vertex). This could be due to the extensive electrochemical damage of the surface and loss of AgSCN or due to the influence of free Ag^+ ions, together with soluble complexes such as $[Ag(SCN)_2]^-$. Furthermore, multiple undesired oxidation products released in solution may later adsorb to the surface and affect the generation of a dense metallic nanostructured network (Fig. S7). Under these extreme oxidation conditions, the fraction of free Ag^+ (unbound to SCN^-) seems to be high enough to generate a reduction peak at about +0.40 V, although the resulting morphology of the silver nanostructures at the end of the two reduction steps (Fig. S7) do not seem to be well correlated with the SERS enhancement of propranolol (Fig. 5B).

Analyzing the Raman spectroelectrochemical data, several issues were observed among the first measurements. The position of the oxidation and reduction peaks of the EC procedure shifted from one experiment to another. Moreover, the SERS signal of propranolol during the SEC experiment presented a very high RSD% of 36% (Fig. S8A), possibly related to the lack of fine control over the applied potential, which is a common problem of commercial SPEs with silver pseudo-RE. To circumvent the uncontrolled adsorption of SCN^- on the silver RE during SEC experiments incriminated for the observed lack of repeatability a fast preconditioning of the pseudo-RE prior to each measurement was performed. As such, 100 μA was applied to the pseudo-RE for 5 s in a solution of 0.1 M $LiClO_4$ and 10 mM KSCN, generating AgSCN

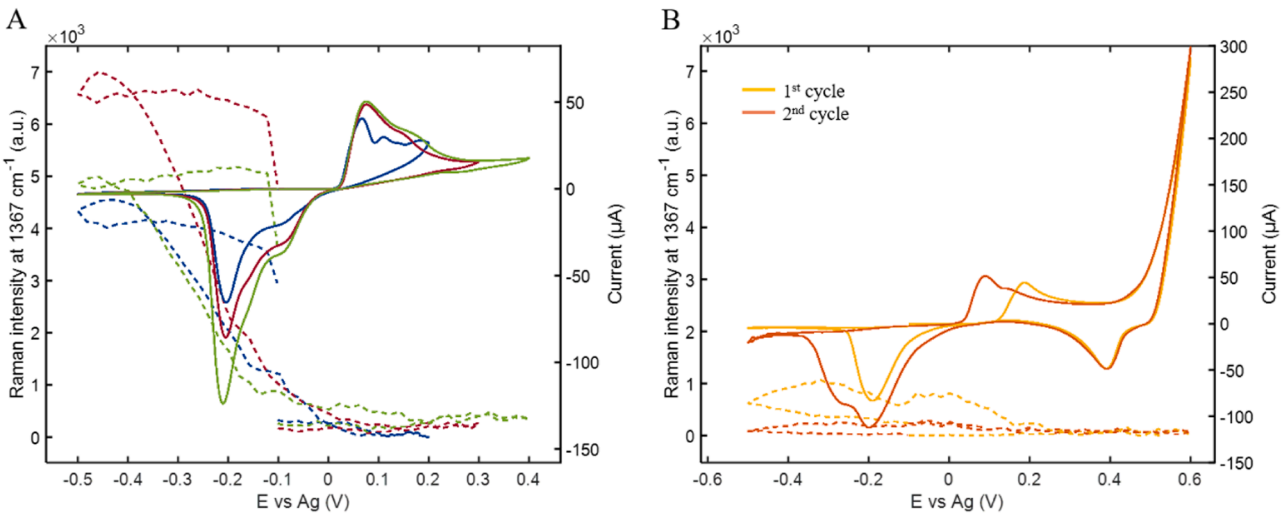

Fig. 5. The second CV cycles and VoltaRamangrams at 1367 cm^{-1} emphasizing different upper vertex potentials with different colors (A) and CV and VoltaRamangram at 1367 cm^{-1} for extreme CV conditions. VoltaRamangrams are represented with dashed line, while EC signals with solid line. Measurement conditions are 0.1 M $LiClO_4$, 10 mM KSCN and 0.5 μM propranolol.

sub-micron particles uniformly covering the electrode's surface (Fig. S9). The resulting Ag/AgSCN RE greatly improved the precision of the recorded EC-SERS signal of propranolol (RSD% = 14%) in the subsequent SEC measurements (Fig. S8B).

3.3. *Effect of subsequent electrode polarization*

The modulation of the EC potential can affect the structure of the double layer, modifying the orientation and adsorption of chemical species in the vicinity of the SERS substrate [36] and leading to changes in enhancement for different vibrational modes of the molecule. However, it should be noted that there is no distinct potential at which a given target molecule's Raman signal is enhanced – this depends on the type of metal substrate [36,37] laser wavelength and on the surrounding medium (pH, electrolyte, concentration, matrix etc.) [1]. Nevertheless, most often, additional SERS enhancement occurs at negative potentials because of the aforementioned mechanisms. The benefits of applying a negative potential during SERS measurement for analytical purposes was previously demonstrated for many molecules such as levofloxacin [38], thiabendazole [39], caffeine [40], paraxanthine [40] and others. For more information on the subject, the reader is directed to reviews on this special topic [1,41].

In this study, a negative potential from –0.10 to –0.90 V in 0.20 V increment was further applied for 20 s right after the in-situ activation of the AgSPEs (Fig. 6A). Once again, the SERS response of propranolol at 1367 cm^{-1} was monitored. Interestingly, an additional nearly two-fold increase (compared to the signal at –0.30 V during activation) of the SERS signal of propranolol at –0.30 V is observed followed by a decrease of the Raman enhancement at lower potential step values (–0.5 to –0.9 V). All the Raman bands in the recorded spectra are simultaneously increased at -0.30 V (Fig. 6B), including the bands at around 225 cm^{-1} and 2114 cm^{-1} related to the chemisorbed SCN^-. Since there are no expected electrochemical reactionsat this potential, a slight plasmonic resonance shift along with molecular reorientation and stabilization of the electrical double-layer through adsorption-desorption processes could be the responsible for the overall increase of the signal. The present results show that the application of a constant negative potential further improves the sensitivity of the studied Ag SERS substrate, in

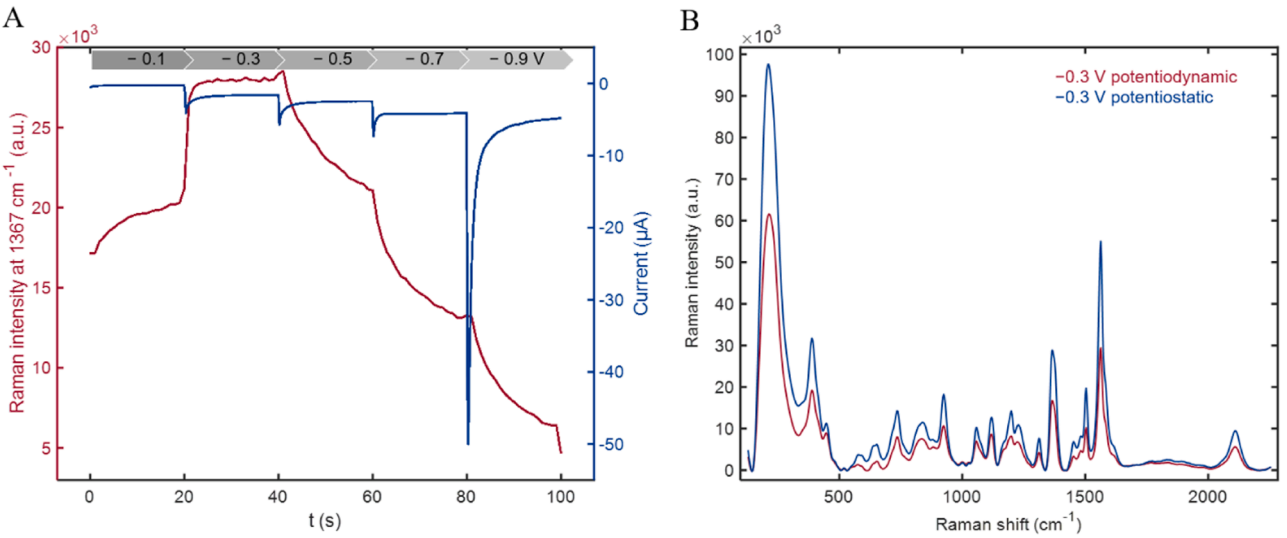

Fig. 6. SERS intensity of propranolol at 1367 cm^{-1} after activation, during a cathodic scan from –0.10 to –0.90 V in 0.20 V increment (A) and comparison between spectra during (red) and after activation (blue) (B). Measurement conditions are 0.1 M $LiClO_4$, 10 mM KSCN and 1 μM propranolol.

comparison with the in-situ performance of the substrate during its electrochemical synthesis.

3.4. Quantitative analysis

The method underwent calibration assessment, where the EC-SERS response was systematically monitored across a range of concentrations spanning from 10 nM to 100 nM, with three replicates performed. The TR-Raman SEC technique allows for the analysis of numerous data points, enabling multivariate regression analysis when needed, for example for more complex samples containing interferents. However, for simplicity, univariate analysis can also be employed. The analysis can be conducted at any stage during the potentiodynamic activation CV method, as long as there is a noticeable SERS enhancement of propranolol or during a stable potential applied to the working electrode following activation.

Within this study, the distinctive Raman band associated with propranolol located at 1367 cm^{-1} was taken into consideration for data analysis during activation (Fig. 7A) and after activation (Fig. 7B), when a fixed potential of –0.30 V (vs. Ag/AgSCN) was applied for 10 s. Linear regression analysis was comparatively performed both with the potentiostatic (Fig. 7C) and the potentiodynamic (Fig. S10) data. A slight improvement in linearity (R^2 0.996 vs. 0.982) is observed in the former case explained by a stabilized system and a more uniform interaction of propranolol with the substrate during a potentiostatic step. Additionally, a 30% increase in the method sensitivity (avg. slope [counts nM^{-1}] ± SD 20.28 ± 4.24 vs. 26.48 ± 3.95) with an estimated LOD of 3.66 nM is recorded, mainly due to favorable plasmonic effects induced by the applied potential. Considering the short integration time (1 s), further lowering of these limits could be potentially attained. Nevertheless, it is worth noting that the current method outperforms in terms of sensitivity and selectivity the previously described SERS (lowest LOD 7.9 nM reported by Levene et al. [42]) and EC [43–46] (lowest LOD 5.6 nM [46]) sensors for propranolol detection. Furthermore, with one exception [37], the reported SERS sensors for propranolol are based on noble metal colloids [42,47] that often encounter reproducibility and stability problems, whereas this study proposes the robust and fast in-situ activation of commercially-available AgSPEs fabricated in a reproducible manner at a large-scale.

As matrix effects often alters the monitored SERS response, the applicability of the developed EC-SERS method has been tested in spiked river and tap water samples. Good recoveries (Table 1, Fig. 7C) were

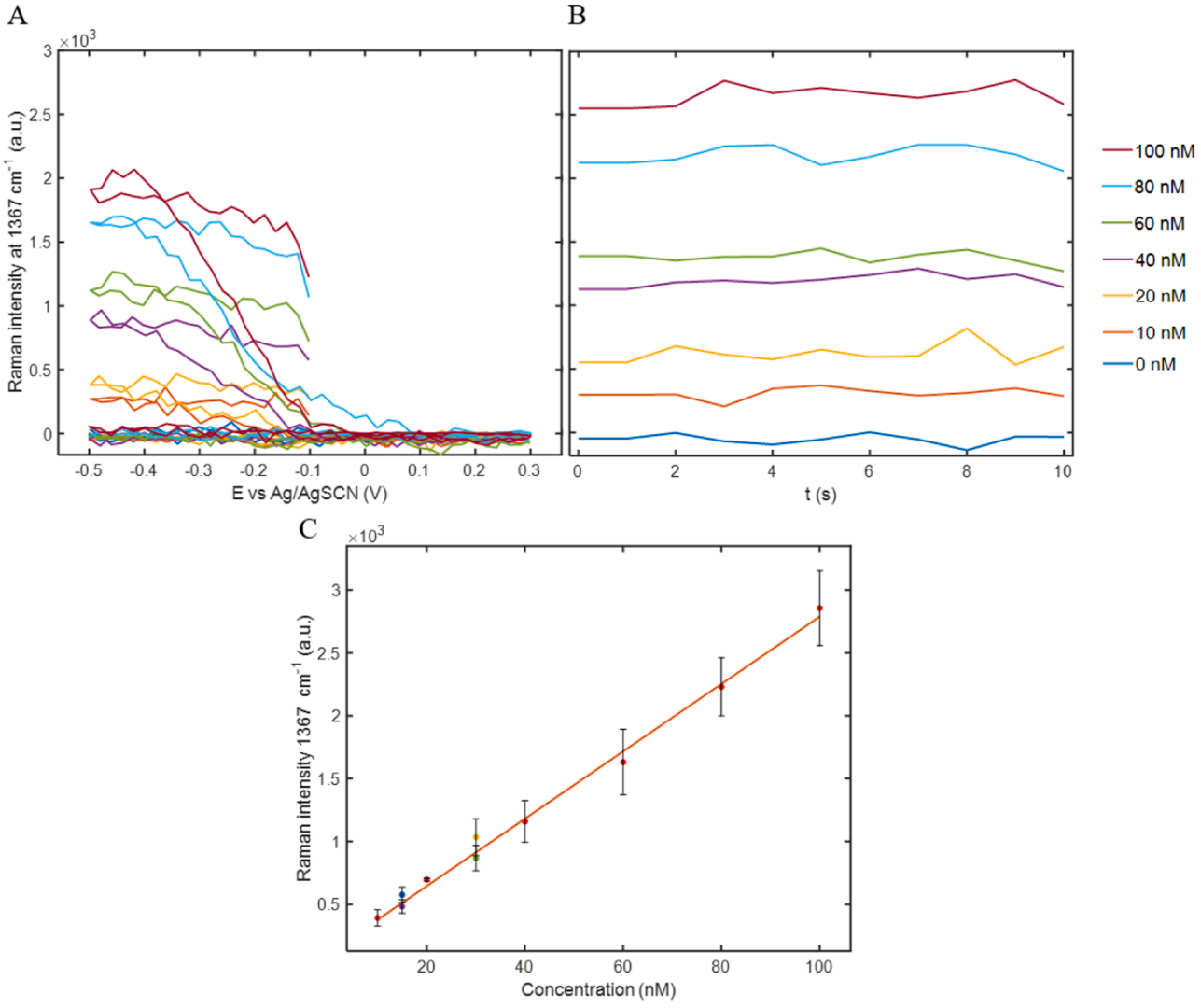

Fig. 7. Evolution of the Raman signal at 1367 cm^{-1} for increasing concentrations of propranolol during the activation procedure (A) and after the activation procedure, at –0.30 V (B). Three measurements were taken for each concentration. Calibration curve using the average Raman intensity at –0.30 V during the potentiostatic step. Blue and purple points represent the river and tap water samples at 15 nM concentrations and green and yellow points represent the river and tap water samples at 30 nM concentration (C).

Table 1
Recovery of propranolol from spiked water samples.

Water sample	Spiked (nM)	Quantified (nM)	Recovery (%)	%RSD*
river	15	16.98	113.25	10.93
tap	15	14.08	93.93	10.88
river	30	28.17	93.91	10.88
tap	30	34.50	115.0	13.32

* n = 3

obtained at two concentration levels (15 and 30 nM propranolol) with RSD% < 13%. The good figures of merit obtained with this methodology for the detection of propranolol in tap and river water suggest that the method is robust to slight changes of common ions such as chloride, which is a classical ion used in the generation of Ag SERS substrates. Nevertheless, it is expectable that samples with high ionic content, such as seawaters, will provide significant interference with the present methodology.

The pH of surface waters tends to vary in the range of 6.5 - 8.5, thus further studies were performed to better understand the influence of pH over the SERS enhancement of propranolol. For this, the Raman signal of propranolol at 1367 cm^{-1} was recorded in Britton Robinson buffer (BRB) solutions of various pHs, containing 10 mM KSCN and 0.1 M $LiClO_4$ (Fig. S11). The SERS enhancement reaches the highest values within the slightly acidic / neutral range (pH = 6 – 7), leveling off significantly in more acidic or alkaline media. In more alkaline media, the neutral form of propranolol, detrimental for SERS enhancement [24], becomes dominant. Furthermore, such media should also be avoided due to the reported chemical instability of the analyte [48] and the initiation of silver hydroxide formation. As propranolol remains in its cationic form (>99%) up to pH 7.6, the observed decrease of the SERS signal below pH 6 may be related to both EM (suboptimal electrode surface nanostructuring) and CM (undesired ionic effects occurring at the surface) enhancement mechanisms, that will require further investigations. Therefore, for a more reproducible SEC quantitative assessment of propranolol levels in real surface waters, samples could be buffered (BRB, pH 6).

4. Conclusions

A novel approach for activating AgSPEs using KSCN as a precipitating agent is proposed for the first time. Through the subsequent oxidation and reduction cycles, thiocyanate guides the progressive build-up of a tridimensional nano-filamentous silver metal network which effectively enhanced the SERS signal of propranolol. This study has pointed out some key factors that play a significant role in the performance of EC-SERS substrates, such as the influence of the potential window and thiocyanate concentration on the final Raman enhancement. Furthermore, the benefits in terms of sensitivity and linearity of an additional potentiostatic step following the potentiodynamic activation were highlighted. The proposed method was successfully employed for quantifying propranolol and analyzing spiked river and tap water samples in the nM range (LOD 3.66 nM). Given its robustness, cost-effectiveness, and rapid activation and measurement times (3 min), the proposed SEC method holds significant potential for monitoring pharmaceutical residues such as propranolol. In future studies, a better understanding of the underlying critical physicochemical mechanisms that occur at the electrode-substrate interface and control the SERS enhancement will be pursued. Also, the applicability of the method to biomedical samples could be assessed, carefully considering the effects of the more complex matrixes. Lastly, it would be interesting to study the reversibility of the adsorption processes of PRNL on the substrate and the possibility of generating recyclable EC-SERS substrates. Nevertheless, preparation of in-situ disposable SERS substrates using electrochemistry is a very interesting strategy to minimize the cost of the analysis.

Funding

Ministerio de Ciencia e Innovación and Agencia Estatal de Investigación (MCIN/AEI/10.13039/501100011033, PID2020-113154RB-C21), Ministerio de Ciencia, Innovación y Universidades (RED2022-134120-T).

CRediT authorship contribution statement

Moldovan Rebeca: Writing – review & editing, Writing – original draft, Visualization, Validation, Methodology, Investigation, Formal analysis, Data curation, Conceptualization. **Bodoki Ede:** Writing – review & editing, Writing – original draft, Visualization, Validation, Supervision, Resources, Project administration, Methodology, Investigation, Funding acquisition, Formal analysis, Data curation, Conceptualization. **Colina Alvaro:** Writing – review & editing, Writing – original draft, Visualization, Validation, Supervision, Software, Resources, Project administration, Methodology, Investigation, Funding acquisition, Formal analysis, Data curation, Conceptualization. **Perez-Estebanez Martin:** Writing – review & editing, Writing – original draft, Visualization, Validation, Software, Methodology, Investigation, Formal analysis, Data curation, Conceptualization. **Heras Aranzazu:** Writing – review & editing, Writing – original draft, Supervision, Resources, Project administration, Investigation, Funding acquisition, Formal analysis.

Declaration of Competing Interest

The authors declare that they have no known competing financial interests or personal relationships that could have appeared to influence the work reported in this paper.

Data Availability

Data will be available at the data repository of the Universidad de Burgos.

Acknowledgements

M. P.-E. acknowledges Junta de Castilla y León and European Social Found for his predoctoral contract.

Appendix A. Supporting information

Supplementary data associated with this article can be found in the online version at doi:10.1016/j.snb.2024.135468.

References

[1] R. Moldovan, E. Vereshchagina, K. Milenko, B.-C. Iacob, A.E. Bodoki, A. Falamas, N. Tosa, C.M. Muntean, C. Farcău, E. Bodoki, Review on combining surface-enhanced Raman spectroscopy and electrochemistry for analytical applications, Anal. Chim. Acta (2021) 339250, https://doi.org/10.1016/j.aca.2021.339250.
[2] D.-Y. Wu, J.-F. Li, B. Ren, Z.-Q. Tian, Electrochemical surface-enhanced Raman spectroscopy of nanostructures, Chem. Soc. Rev. 37 (2008) 1025–1041, https://doi.org/10.1039/b707872m.
[3] Z. Zhu, W.V. Espulgar, H. Yoshikawa, M. Saito, B. Fan, X. Dou, E. Tamiya, Electrochemically modulated surface-enhanced Raman spectra of aminoglutethimide (AGI) on a Ag-sputtered electrode, Bull. Chem. Soc. Jpn. 91 (2018) 1579–1585, https://doi.org/10.1246/bcsj.20180172.
[4] C.L. Brosseau, A. Colina, J.V. Perales-Rondon, A.J. Wilson, P.B. Joshi, B. Ren, X. Wang, Electrochemical surface-enhanced Raman spectroscopy, Nat. Rev. Methods Prim. 3 (2023) 79, https://doi.org/10.1038/s43586-023-00263-6.
[5] A.V. Markin, A.I. Arzhanukhina, N.E. Markina, I.Y. Goryacheva, Analytical performance of electrochemical surface-enhanced Raman spectroscopy: a critical review, TrAC Trends Anal. Chem. 157 (2022) 116776, https://doi.org/10.1016/j.trac.2022.116776.
[6] D. Martín-Yerga, A. Pérez-Junquera, M.B. González-García, J.V. Perales-Rondon, A. Heras, A. Colina, D. Hernández-Santos, P. Fanjul-Bolado, Quantitative Raman spectroelectrochemistry using silver screen-printed electrodes, Electrochim. Acta 264 (2018) 183–190, https://doi.org/10.1016/j.electacta.2018.01.060.

[7] D. Martín-Yerga, A. Pérez-Junquera, M.B. González-García, D. Hernández-Santos, P. Fanjul-Bolado, Towards single-molecule in situ electrochemical SERS detection with disposable substrates, Chem. Commun. 54 (2018) 5748–5751, https://doi.org/10.1039/C8CC02069H.
[8] C.E. Ott, M. Perez-Estebanez, S. Hernandez, K. Kelly, K.A. Dalzell, M.J. Arcos-Martinez, A. Heras, A. Colina, L.E. Arroyo, Forensic identification of fentanyl and its analogs by electrochemical-surface enhanced Raman spectroscopy (EC-SERS) for the screening of seized drugs of abuse, Front. Anal. Sci. 2 (2022), https://doi.org/10.3389/frans.2022.834820.
[9] C.N. Hernández, D. Martín-Yerga, M.B. González-García, D. Hernández-Santos, P. Fanjul-Bolado, Evaluation of electrochemical, UV/VIS and Raman spectroelectrochemical detection of Naratriptan with screen-printed electrodes, Talanta 178 (2018) 85–88, https://doi.org/10.1016/j.talanta.2017.09.004.
[10] W. Cheuquepan, S. Hernandez, M. Perez-Estebanez, L. Romay, A. Heras, A. Colina, Electrochemical generation of surface enhanced Raman scattering substrates for the determination of folic acid, J. Electroanal. Chem. 896 (2021) 115288, https://doi.org/10.1016/j.jelechem.2021.115288.
[11] M. Perez-Estebanez, W. Cheuquepan, M. Huidobro, J.V. Cuevas, S. Hernandez, A. Heras, A. Colina, Raman spectroelectrochemical determination of clopyralid in tap water, Microchem. J. 183 (2022) 108018, https://doi.org/10.1016/j.microc.2022.108018.
[12] X. Li, A.A. Gewirth, Potential-dependent reorientation of thiocyanate on Au electrodes, J. Am. Chem. Soc. 125 (2003) 11674–11683, https://doi.org/10.1021/ja0363112.
[13] P. Wang, H. Li, C. Cui, J. Jiang, In situ surface-enhanced Raman spectroscopy study of thiocyanate ions adsorbed on silver nanoparticles under high pressure, Chem. Phys. 516 (2019) 1–5, https://doi.org/10.1016/j.chemphys.2018.08.029.
[14] A.A. Godoy, F. Kummrow, P.A.Z. Pamplin, Occurrence, ecotoxicological effects and risk assessment of antihypertensive pharmaceutical residues in the aquatic environment - a review, Chemosphere 138 (2015) 281–291, https://doi.org/10.1016/j.chemosphere.2015.06.024.
[15] L.H.M.L.M. Santos, A.N. Araújo, A. Fachini, A. Pena, C. Delerue-Matos, M.C.B.S. M. Montenegro, Ecotoxicological aspects related to the presence of pharmaceuticals in the aquatic environment, J. Hazard. Mater. 175 (2010) 45–95, https://doi.org/10.1016/j.jhazmat.2009.10.100.
[16] J.P. Sumpter, T.J. Runnalls, R.L. Donnachie, S.F. Owen, A comprehensive aquatic risk assessment of the beta-blocker propranolol, based on the results of over 600 research papers, Sci. Total Environ. 793 (2021) 148617, https://doi.org/10.1016/j.scitotenv.2021.148617.
[17] Y. Yang, Y. Cao, J. Jiang, X. Lu, J. Ma, S. Pang, J. Li, Y. Liu, Y. Zhou, C. Guan, Comparative study on degradation of propranolol and formation of oxidation products by UV/H2O2 and UV/persulfate (PDS), Water Res 149 (2019) 543–552, https://doi.org/10.1016/j.watres.2018.08.074.
[18] T. Deblonde, C. Cossu-Leguille, P. Hartemann, Emerging pollutants in wastewater: a review of the literature, Int. J. Hyg. Environ. Health 214 (2011) 442–448, https://doi.org/10.1016/j.ijheh.2011.08.002.
[19] M. Yi, Q. Sheng, Q. Sui, H. Lu, β-blockers in the environment: distribution, transformation, and ecotoxicity, Environ. Pollut. 266 (2020) 115269, https://doi.org/10.1016/j.envpol.2020.115269.
[20] L.N. Nikolai, E.L. McClure, S.L. MacLeod, C.S. Wong, Stereoisomer quantification of the β-blocker drugs atenolol, metoprolol, and propranolol in wastewaters by chiral high-performance liquid chromatography–tandem mass spectrometry, J. Chromatogr. A. 1131 (2006) 103–109, https://doi.org/10.1016/j.chroma.2006.07.033.
[21] A.M. Robinson, S.G. Harroun, J. Bergman, C.L. Brosseau, Portable electrochemical surface-enhanced raman spectroscopy system for routine spectroelectrochemical analysis, Anal. Chem. 84 (2012) 1760–1764, https://doi.org/10.1021/ac2030078.
[22] F. Olmo-Alonso, J. Garoz-Ruiz, A. Heras, A. Colina, Normal or parallel configuration in spectroelectrochemistry? Bidimensional spectroelectroanalysis in presence of an antioxidant compound, J. Electroanal. Chem. 935 (2023) 117333, https://doi.org/10.1016/j.jelechem.2023.117333.
[23] Metrohm DropSens: Screen-Printed electrodes, (2018). ⟨https://www.dropsens.com/en/pdfs_productos/new_brochures/c013_010.pdf⟩ (accessed October 3, 2023).
[24] R. Stiufiuc, C. Iacovita, C.M. Lucaciu, G. Stiufiuc, R. Nicoara, M. Oltean, V. Chis, E. Bodoki, Adsorption geometry of propranolol enantiomers on silver nanoparticles, J. Mol. Struct. 1031 (2013) 201–206, https://doi.org/10.1016/j.molstruc.2012.10.001.
[25] A. Farcas, I. Cristian, E. Vinţeler, V. Chis, R. Stiufiuc, M. Lucaciu, The influence of molecular structure modifications on vibrational properties of some beta blockers: a combined Raman and DFT study, J. Spectrosc. 2016 (2016) 1–9, https://doi.org/10.1155/2016/3137140.
[26] K. Wonner, M.V. Evers, K. Tschulik, The electrochemical dissolution of single silver nanoparticles enlightened by hyperspectral dark-field microscopy, Electrochim. Acta 301 (2019) 458–464, https://doi.org/10.1016/j.electacta.2019.01.129.
[27] V. Brasiliense, A.N. Patel, A. Martinez-Marrades, J. Shi, Y. Chen, C. Combellas, G. Tessier, F. Kanoufi, Correlated electrochemical and optical detection reveals the chemical reactivity of individual silver nanoparticles, J. Am. Chem. Soc. 138 (2016) 3478–3483, https://doi.org/10.1021/jacs.5b13217.
[28] I.– A. Stoian, B.-C. Iacob, J.P. Prates Ramalho, I.O. Marian, V. Chiş, E. Bodoki, R. Oprean, A chiral electrochemical system based on l-cysteine modified gold nanoparticles for propranolol enantiodiscrimination: electroanalysis and computational modelling, Electrochim. Acta 326 (2019) 134961, https://doi.org/10.1016/j.electacta.2019.134961.
[29] H.-L. Zhu, G.-F. Liu, F.-J. Meng, Refinement of the crystal structure of silver (I) thiocyanate, AgSCN, Z. Für Krist. - N. Cryst. Struct. 218 (2003), https://doi.org/10.1524/ncrs.2003.218.jg.285.
[30] R.P. Cooney, E.S. Reid, M. Fleischmann, P.J. Hendra, Thiocyanate adsorption and corrosion at silver electrodes. A Raman spectroscopic study, J. Chem. Soc. Faraday Trans. 73 (1977) 1691–1698, https://doi.org/10.1039/F19777301691.
[31] P. Gans, J.B. Gill, M. Griffin, Spectrochemistry of solutions. Part 5. — Raman spectroscopic study of the coordination of silver(I) ions in liquid ammonia by thiocyanate ions, J. Chem. Soc. Faraday Trans. 74 (1978) 432–439, https://doi.org/10.1039/F19787400432.
[32] R.M. Onorato, D.E. Otten, R.J. Saykally, Adsorption of thiocyanate ions to the dodecanol/water interface characterized by UV second harmonic generation, Proc. Natl. Acad. Sci. USA 106 (2009) 15176–15180, https://doi.org/10.1073/pnas.0904800106.
[33] N. Leopold, A. Stefancu, K. Herman, I.S. Tódor, S.D. Iancu, V. Moisoiu, L. F. Leopold, The role of adatoms in chloride-activated colloidal silver nanoparticles for surface-enhanced Raman scattering enhancement, Beilstein J. Nanotechnol. 9 (2018) 2236–2247, https://doi.org/10.3762/bjnano.9.208.
[34] M. Muniz-Miranda, G. Sbrana, Evidence for surface Ag+ complex formation by an anion-induced effect in the SER spectra of phthalazine adsorbed on silver sols, J. Raman Spectrosc. 27 (1996) 105–110, https://doi.org/10.1002/(SICI)1097-4555(199602)27:2<105::AID-JRS933>3.0.CO;2-L.
[35] E. Kämmer, K. Olschewski, P. Rösch, K. Weber, D. Cialla-May, J. Popp, High-throughput screening of measuring conditions for an optimized SERS detection, J. Raman Spectrosc. 47 (2016) 1003–1011, https://doi.org/10.1002/jrs.4849.
[36] M. Dendisová, Z. Němečková, M. Člupek, V. Prokopec, EC-SERS study of phenolic acids sorption behavior on Au, Ag and Cu substrates – Effect of applied potential and metal used, Appl. Surf. Sci. 470 (2019) 716–723, https://doi.org/10.1016/j.apsusc.2018.11.120.
[37] C.M. Muntean, D. Cuibus, S. Boca, A. Falamas, N. Tosa, I.A. Brezeştean, A. Bende, L. Barbu-Tudoran, R. Moldovan, E. Bodoki, C. Farcău, Gold vs. silver colloidal nanoparticle films for optimized SERS detection of propranolol and electrochemical-SERS analyses, Biosensors 13 (2023), https://doi.org/10.3390/bios13050530.
[38] S.D. Bindesri, D.S. Alhatab, C.L. Brosseau, Development of an electrochemical surface-enhanced Raman spectroscopy (EC-SERS) fabric-based plasmonic sensor for point-of-care diagnostics, Analyst 143 (2018) 4128–4135, https://doi.org/10.1039/C8AN01117F.
[39] R. Moldovan, K. Milenko, E. Vereshchagina, B.-C. Iacob, K. Schneider, C. Farcău, E. Bodoki, EC-SERS detection of thiabendazole in apple juice using activated screen-printed electrodes, Food Chem. 405 (2023) 134713, https://doi.org/10.1016/j.foodchem.2022.134713.
[40] M. Velička, E. Zacharovas, S. Adomavičiūtė, V. Šablinskas, Detection of caffeine intake by means of EC-SERS spectroscopy of human saliva, Spectrochim. Acta Part A Mol. Biomol. Spectrosc. 246 (2021) 118956, https://doi.org/10.1016/j.saa.2020.118956.
[41] J. Garoz-Ruiz, J.V. Perales-Rondon, A. Heras, A. Colina, Spectroelectrochemical sensing: current trends and challenges, Electroanalysis 31 (2019) 1254–1278, https://doi.org/10.1002/elan.201900075.
[42] C. Levene, E. Correa, E.W. Blanch, R. Goodacre, Enhancing surface enhanced Raman scattering (SERS) detection of propranolol with multiobjective evolutionary optimization, Anal. Chem. 84 (2012) 7899–7905, https://doi.org/10.1021/ac301647a.
[43] A. Ambrosi, R. Antiochia, L. Campanella, R. Dragone, I. Lavagnini, Electrochemical determination of pharmaceuticals in spiked water samples, J. Hazard. Mater. 122 (2005) 219–225, https://doi.org/10.1016/j.jhazmat.2005.03.011.
[44] A. Dehnavi, A. Soleymanpour, Titanium dioxide/multi-walled carbon nanotubes composite modified pencil graphite sensor for sensitive voltammetric determination of propranolol in real samples, Electroanalysis (2020), https://doi.org/10.1002/elan.202060132.
[45] Y. Liu, J. Strutwolf, D.W.M. Arrigan, Ion-transfer voltammetric behavior of propranolol at nanoscale liquid–liquid interface arrays, Anal. Chem. 87 (2015) 4487–4494, https://doi.org/10.1021/acs.analchem.5b00461.
[46] A.A. Khorshed, M. Khairy, C.E. Banks, Electrochemical determination of antihypertensive drugs by employing costless and portable unmodified screen-printed electrodes, Talanta 198 (2019) 447–456, https://doi.org/10.1016/j.talanta.2019.01.117.
[47] A. Subaihi, L. Almanqur, H. Muhamadali, N. AlMasoud, D.I. Ellis, D.K. Trivedi, K. A. Hollywood, Y. Xu, R. Goodacre, Rapid, accurate, and quantitative detection of propranolol in multiple human biofluids via surface-enhanced Raman scattering, Anal. Chem. 88 (2016) 10884–10892, https://doi.org/10.1021/acs.analchem.6b02041.
[48] L. Yin, R. Ma, B. Wang, H. Yuan, G. Yu, The degradation and persistence of five pharmaceuticals in an artificial climate incubator during a one year period, RSC Adv. 7 (2017) 8280–8287, https://doi.org/10.1039/C6RA28351A.

Rebeca Moldovan is a PhD student in Analytical Chemistry at "Iuliu Haţieganu" University of Medicine and Pharmacy, Cluj-Napoca, Romania. Her research is currently focused on developing spectroelectrochemical sensors for analytical purposes and investigating strategies for selective capturing of analytes on SERS substrates.

Martin Perez-Estebanez is a postdoctoral researcher at the Universidad de Burgos, Spain. His interests are focused on the study of new SERS substrates based on dielectric and semiconductor materials and its application for analysis of electrochemical interfaces and for the development of analytical applications

Aranzazu Heras is full professor in the Department of Chemistry at the Universidad de Burgos (Spain). Her research interests include different aspects related to spectroelectrochemistry (UV-Vis-NIR, photoluminescence, Raman), from the design and development of new devices to applications of these techniques in analysis, characterization of organic, inorganic and nanomaterials, and in the study of different reaction mechanisms.

Ede Bodoki is an appointed professor at the Analytical Chemistry Department, Faculty of Pharmacy within the University of Medicine & Pharmacy "Iuliu Hatieganu" Cluj-Napoca, Romania. He is leading the group of molecular imprinting and functional polymers. Prof. Bodoki has a substantial expertise in a broad spectrum of analytical tools applied in pharmaceutical, environmental and biomedical analysis, such as separation sciences, involving liquid chromatographic (HPTLC, HPLC) and capillary electrophoretic techniques, molecularly imprinted polymers as biomimetic recognition platforms and drug delivery systems, (bio)electroanalysis (EC) using various molecular recognition elements in the development of chemo/biosensors, several hyphenated analytical techniques (EC-HPLC/MS, spectroelectrochemistry, etc.) and chemometry (experimental design, multivariate data analysis).

Alvaro Colina is full professor in the Department of Chemistry of the Universidad de Burgos, Spain. His research interests are devoted to the development of new multiresponse instrumental techniques. Particularly, he has developed a number of different spectroelectrochemistry techniques and devices that have been applied in the characterization materials, study of reaction mechanisms and for analytical purposes. In the last years, he is involved in the development of new analytical strategies for EC-SERS